

## Tuning Surface Wettability and Porosity of ZnO/Geopolymer Composite Membranes from Coal Fly Ash through H<sub>2</sub>O<sub>2</sub> as Pore-Forming Agent

Rendy Muhamad Iqbal<sup>a\*</sup>, Siswo Siswo<sup>a)</sup>, Erwin Prasetya Toepak<sup>a)</sup>, Hamzah Fansuri<sup>b)</sup>, Muhammad ‘Adli Nor Azman<sup>c)</sup>, Yusuf Wibisono<sup>d)</sup>, Sri Wardhani<sup>e)</sup>, Deni Shidqi Khaerudini<sup>f)</sup>

<sup>a)</sup> Department of Chemistry, Faculty of Mathematics and Natural Sciences, Universitas Palangka Raya, Palangka Raya 73111, Indonesia

<sup>b)</sup> Department of Chemistry, Faculty of Science and Data Analytics, Institut Teknologi Sepuluh Nopember, Surabaya 60111, Indonesia

<sup>c)</sup> World Premier International Center for Materials Nanoarchitectonics (WPI-MANA) National Institute of Materials Science (NIMS), 1-1 Namiki, Tsukuba, Ibaraki 305-0044, Japan

<sup>d)</sup> Department of Bioprocess Engineering, Faculty of Agricultural Technology, Universitas Brawijaya, Malang 65145, Indonesia

<sup>e)</sup> Department of Chemistry, Faculty of Mathematics and Natural Sciences, Universitas Brawijaya, Malang 65145, Indonesia

<sup>f)</sup> Research Centre for Energy Conversion and Conservation, National Research and Innovation Agency (BRIN), KST BJ Habibie, Tangerang Selatan, Indonesia

<sup>\*</sup> Corresponding Author: [iqbal.rm@fmipa.upr.ac.id](mailto:iqbal.rm@fmipa.upr.ac.id)

DOI: <https://doi.org/10.33751/helium.v6i1.51>

Article history: received: 26-02-2026; revised: 13-04-2026; accepted: 22-04-2026; published: 02-06-2026

### ABSTRACT.

The development of geopolymer membranes from industrial by-products offers a sustainable approach for water purification. In this study, ZnO/geopolymer membranes were prepared from coal fly ash, with hydrogen peroxide (H<sub>2</sub>O<sub>2</sub>) used as a pore-forming agent to regulate porosity and surface wettability. The influence of H<sub>2</sub>O<sub>2</sub> concentration (0-6 wt%) on membrane physicochemical properties was systematically evaluated. FTIR analysis confirmed the formation of sodium aluminosilicate hydrate (N-A-S-H) gel and the incorporation of ZnO through the presence of Si-O-Zn and Zn-O bands. SEM images showed that increasing H<sub>2</sub>O<sub>2</sub> concentration changed the initially dense structure into a rougher and more porous surface due to oxygen bubble generation during curing. ZnO addition enhanced surface roughness and functionality, while H<sub>2</sub>O<sub>2</sub> improved pore connectivity. The water contact angle decreased from 21.63° in the pristine geopolymer to below 15° in the membrane with 6 wt% H<sub>2</sub>O<sub>2</sub>, indicating greater hydrophilicity. Porosity also increased from about 10% to 50%. These results demonstrate that ZnO incorporation combined with controlled H<sub>2</sub>O<sub>2</sub> addition effectively tailors membrane wettability and pore structure, making the composite promising for sustainable water filtration.

**Keywords:** fly ash, geopolymer, inorganic chemistry, membrane

### 1. Introduction

The advancement of water purification technology has led to an increasing demand for clean, safe water resources. Membrane technology is one of the most important innovations since it allows for efficient and widespread use of water [1]. However, many conventional membranes, such as synthetic polymers, have limitations in terms of durability, cleanliness, and fouling, which reduce filtering efficiency. Because of this, developing new materials

that are more stable and long-lasting is critical. One popular alternative is geopolymer membranes, which are inorganic materials based on alumina-silicate that have high mechanical strength, excellent stability, and may be made from by-products from coal combustion [2]. Aside from providing good performance, geopolymer adheres to the principle of the circular economy by using industrial waste as a raw material for water pollution control.

Although geopolymer membranes have various advantages, including strong chemical and thermal stability and tolerance to extreme temperatures, their usage in water filtration is still limited [3,4]. The main issues are low porosity and restricted surface hydrophilicity, which cause low water flux and an increased danger of fouling when utilized for wastewater treatment that might be contained complexes compound, which easily cling to membrane pores, causing clogging and lowering filtration effectiveness. Controlling the pore structure is thus an important part of geopolymer membrane engineering to establish a balance between permeability and fouling resistance.

The use of hydrogen peroxide ( $H_2O_2$ ) as a pore-forming agent is a significant and promising strategy. During geopolymerization,  $H_2O_2$  can generate oxygen bubbles through thermal or catalytic breakdown, resulting in an open and equally distributed pore network inside the matrix. Variations in  $H_2O_2$  concentration can control pore size and volume, directly affecting the membrane's physical properties such as density, permeability, and water uptake [5]. Optimizing the usage of  $H_2O_2$  allows for high porosity membranes while preserving mechanical strength. This is significant because suitably large and continuously connected pores will allow for more effective water transport while preserving filtration selectivity.

Previous studies have used  $H_2O_2$  as a pore-forming agent in ceramic and geopolymer materials [6, 7]. However, studies combining this method with active metal oxide modifications like ZnO are still quite rare. Then, combining pore engineering with surface alteration can result in considerable synergistic effects.  $H_2O_2$ 's open pore structure enhances the dispersion of ZnO particles in the geopolymer matrix, leading to increased active surface area and more effective photocatalytic interactions with organic contaminants. Furthermore, the addition of ZnO can increase the membrane's hydrophilic qualities, reduce the accumulation of organic compounds in the pores, and give self-cleaning capabilities via a photocatalytic mechanism under light irradiation [8].

In addition, this study focuses on systematically investigating the effect on the physicochemical properties of ZnO/geopolymer

membranes derived from coal fly ash. Particular attention is given to understanding how  $H_2O_2$  influences pore information, surface morphology, and structural characteristics. This work aims to provide fundamental insights into the design and optimization of geopolymer-based membrane materials.

## 2. Methods

This study describes the fabrication of ZnO/geopolymer composite membranes using coal fly ash and hydrogen peroxide as a pore-forming agent, followed by physicochemical characterization, including FTIR, XRD, SEM, water contact angle, and porosity analysis.

### 2.1 Materials and Instruments

The materials used in this study included fly ash obtained from the Pulang Pisau coal-fired power plant, sodium hydroxide (NaOH, EMSURE® ISO grade), aluminum hydroxide ( $Al(OH)_3$ , EMSURE®), sodium silicate ( $Na_2SiO_3$ , E'MERCK technical grade), zinc oxide (ZnO, Merck), hydrogen peroxide ( $H_2O_2$ , 50 wt%), sulfuric acid ( $H_2SO_4$ , 37%, SMART-LAB analytical grade).

### 2.2 Fabrication of geopolymer membrane composite from coal fly ash

The ZnO/Geopolymer membrane mixture is prepared through mixing 65 grams of Pulang Pisau fly ash with 0.85 grams of aluminum hydroxide ( $Al(OH)_3$ ), then adding the previously prepared activating base solution and stirring for five minutes using a mixer. Hydrogen peroxide ( $H_2O_2$ ), a pore-forming agent that has been diluted to a concentration of 5% with variations of 0, 2, 4, and 6 wt% of the total weight of the geopolymer material, was added after stirring until it was evenly distributed. According to earlier research, three grams of zinc dioxide (ZnO) were added and swirled for two minutes after a variety of hydrogen peroxide ( $H_2O_2$ ) was added and mixed for two minutes to ensure even distribution. After that, zinc dioxide (ZnO) was added as an anti-fouling agent to enhance the functionality of geopolymer membranes. Once everything was well blended, the slurry was transferred to a disk-shaped mould that was 4.3 cm in

diameter and 0.5 cm in height. The samples were placed in a sealed plastic container and cured at ambient temperature ( $27 \pm 2^\circ\text{C}$ ) for 30 days under uncontrolled humidity conditions, while minimizing moisture loss by maintaining a closed environment.

The samples with various  $\text{H}_2\text{O}_2$  concentrations of 0, 2, 4, and 6 wt% were denoted as ZGH0, ZGH2, ZGH4, and ZGH6, respectively. Then, the schematic fabrication process of the geopolymer membrane composite was visualized in Figure 1.

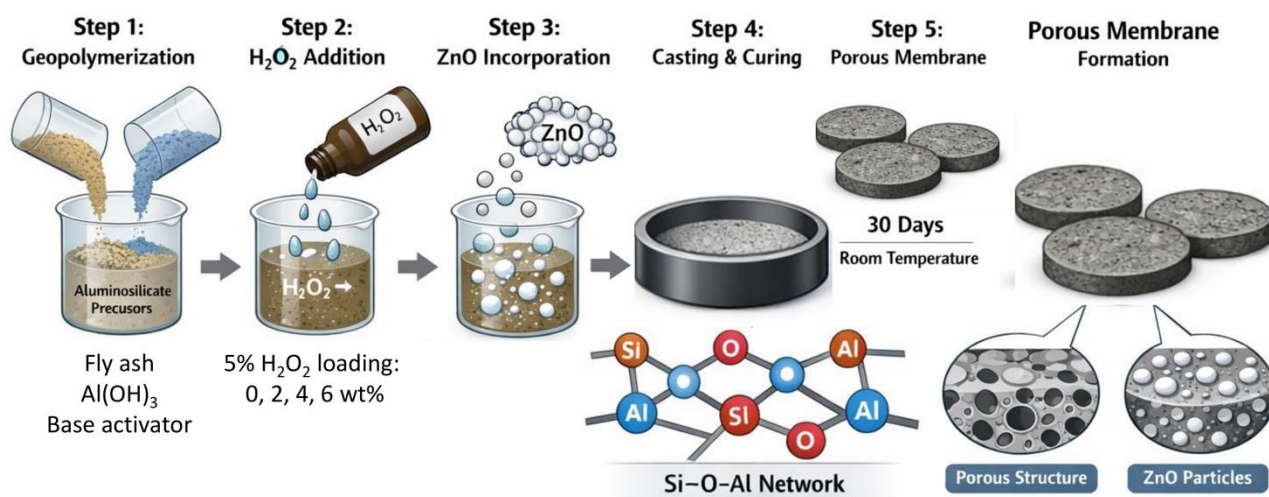


Figure 1. Schematic illustration of the preparation of ZnO/geopolymer composite membranes derived from coal fly ash using  $\text{H}_2\text{O}_2$  as a pore-forming agent.

## 2.3 Membrane Characterization

In order to ascertain the physicochemical characteristics of the manufactured membrane, a geopolymer and ZnO/geopolymer membrane composite was conducted utilizing X-Ray Diffraction (XRD), Scanning Electron Microscope (SEM), Fourier Transform Infrared (FTIR), and Water Contact Angle (WCA). Afterwards, membrane porosity was determined using Archimedes' approach. This procedure is carried out by measuring the surface area of the membrane ( $A$ ), height ( $h$ ), and then dipping the membrane into water for 30 minutes. Dry mass ( $W_d$ ) and membrane mass after immersion ( $W_w$ ) were weighed using an analytical balance. This stage was repeated 3 times to reduce the occurrence of measurement errors. Next, the porosity calculation is shown in equation 1 [9].

$$\text{Porosity (\%)} = \frac{W_w - W_d}{A \times h} \times 100 \quad \text{Eq. 1}$$

## 3. Results and Discussion

The FTIR spectra of fly ash, geopolymer membrane, and ZnO/geopolymer membrane modified with  $\text{H}_2\text{O}_2$  as pore-forming agent (ZGH6) are introduced in Figure 2. The spectrum of the raw fly ash demonstrated a broad and intense absorption band around  $1110 \text{ cm}^{-1}$ , which corresponds to the asymmetric stretching vibration of T-O-T, where T is Si or Al, which is characteristic of aluminosilicate phases such as quartz and mullite. The bands at approximately  $794$  and  $461 \text{ cm}^{-1}$  were also attributed to Si-O symmetric stretching and Si-O-Al bending vibrations, respectively. The relatively low intensity and broadness of these bands indicate the presence of both crystalline and amorphous aluminosilicate phases in the fly ash, which act as precursors in the geopolymerization process [10, 11].

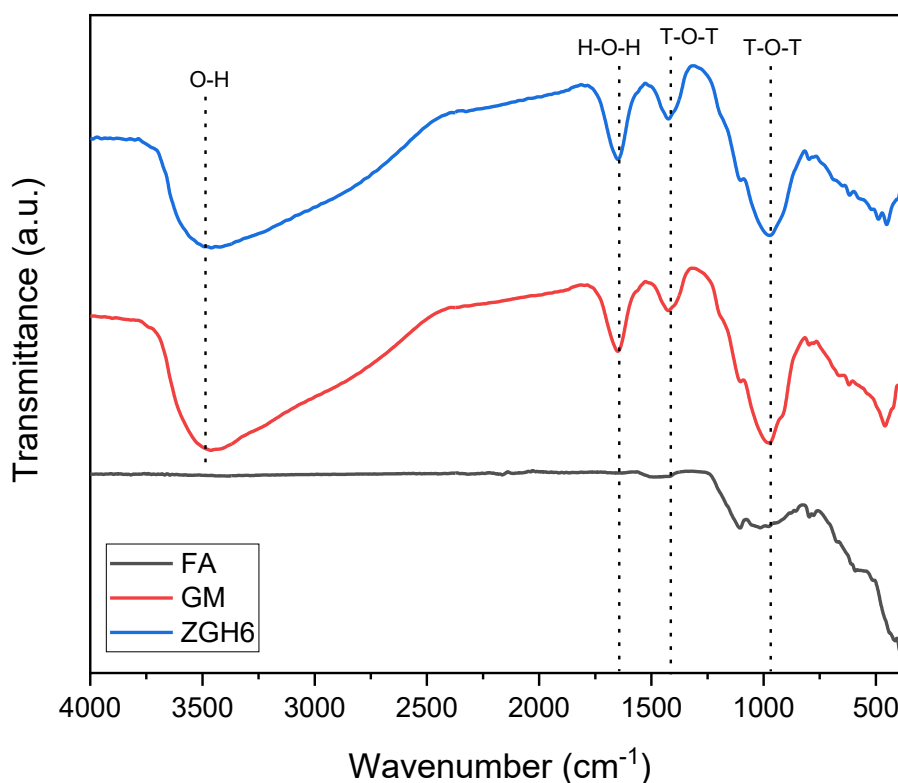


Figure 2. FTIR spectra of fly ash (FA), geopolymer (GM), and ZnO/geopolymer membrane composite (ZGH6)

After the geopolymerization reaction, the FTIR spectrum of the geopolymer membrane demonstrated a significant shift of the main Si-O-T (T = Si or Al) asymmetric stretching band from  $1110\text{ cm}^{-1}$  to around  $791\text{ cm}^{-1}$ . This shift indicates the dissolution and reorganization of the original aluminosilicate network into a new amorphous three-dimensional geopolymeric framework, where Si and Al atoms are tetrahedrally coordinated and linked by oxygen bridges. This transformation reflects the successful formation of sodium aluminosilicate hydrate (N-A-S-H) gel, which is responsible for the binding matrix in the geopolymer. Furthermore, the appearance of absorption bands near  $1641\text{ cm}^{-1}$  and  $3442\text{ cm}^{-1}$  corresponds to the bending and stretching vibrations of H-O-H and O-H groups, respectively, originating from physically adsorbed water and hydroxyl species within the geopolymer structure [10, 11, 12, 13]. These features are typical of geopolymer cured under ambient conditions, where residual moisture and surface hydroxylation contribute to the material's hydrophilic nature.

Upon the incorporation of ZnO and modification with 6 wt%  $\text{H}_2\text{O}_2$ , several notable changes were observed. The O-H stretching band around  $3442\text{ cm}^{-1}$  becomes more pronounced, suggesting that the  $\text{H}_2\text{O}_2$ -assisted synthesis promotes the formation of additional hydroxyl groups on the membrane surface, possibly due to particle oxidation and increased surface area. The Si-O-T stretching band slightly shifts and broadens, indicating chemical interaction between ZnO and the aluminosilicate network, likely through Si-O-Zn or Al-O-Zn linkages [10, 12]. Moreover, the presence of a distinct band at around  $461\text{ cm}^{-1}$  is characteristic of Zn-O stretching vibrations, confirming the successful deposition of ZnO on the geopolymer surface. Another indicator was the broader peak in the fingerprint area for ZGH6, which caused overlapping vibrational modes and increased structural heterogeneity, likely arising from the interaction between ZnO and the aluminosilicate gel network. The ZnO incorporation can modify the surface chemistry and enhance membrane functionalities such as hydrophilicity, photocatalytic activity, and antibacterial behavior.

Figure 3 shows the XRD patterns, which provide insight into the phase composition and structural evolution from raw fly ash (FA) to geopolymer membrane (GM), and further to ZnO-incorporated geopolymer membrane (ZGH6). FA exhibits a complex diffraction pattern dominated by a broad amorphous hump centered at approximately  $2\theta = 20\text{--}35^\circ$ , which is characteristic of vitreous aluminosilicate glass commonly found in coal-derived fly ash [14]. Superimposed on this amorphous

background are several sharp crystalline peaks, which can be attributed to residual mineral phases such as quartz (Q,  $\text{SiO}_2$ ) and mullite (M,  $\text{Al}_6\text{Si}_2\text{O}_{13}$ ). The intense peak around  $2\theta \approx 26.6^\circ$  corresponds to the (101) plane of quartz, while weaker reflections at higher angles indicate the presence of mullite. These crystalline phases are chemically stable and largely inert during alkaline activation, serving mainly as fillers within the geopolymer matrix [14].

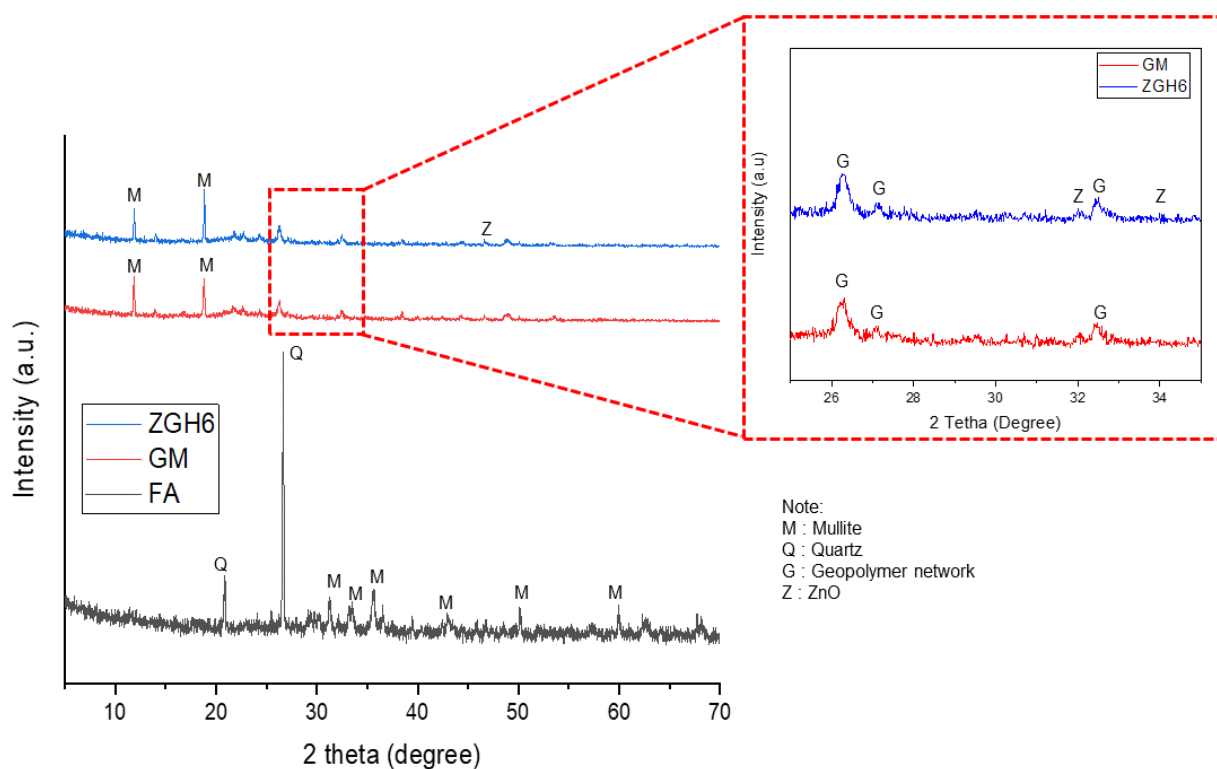


Figure 3. Diffractogram of geopolymer and ZnO/geopolymer membrane composite

After alkaline activation and membrane formation, the GM shows a significant structural transformation. The XRD pattern of GM is characterized by a broadened and more pronounced amorphous, typically shifted toward  $2\theta \approx 25\text{--}40^\circ$ , indicating the formation of a new amorphous sodium aluminosilicate hydrate (N-A-S-H) geopolymer gel, representing a geopolymer network (G) [15]. This shift and broadening confirm the dissolution of reactive Si and Al species from fly ash and their subsequent polycondensation into a three-dimensional

geopolymeric network. Meanwhile, the characteristic peaks of quartz and mullite remain visible as residual raw material, suggesting that these crystalline phases persist but are partially embedded within the amorphous geopolymer matrix [16]. The dominance of the amorphous phase is a key indicator of successful geopolymerization and is beneficial for membrane applications due to improving the structural homogeneity and mechanical integrity.

In addition, two relatively weak but distinguishable peaks observed below  $2\theta \approx 20^\circ$ ,

labelled as M, become more apparent in GM and ZGH6 compared to FA. These peaks are attributed to residual mullite, whose enhanced visibility is associated with the reduction of overlapping phases and background complexity after geopolymerization. This suggests that while the amorphous fraction of FA actively participates in gel formation, the crystalline mullite phase remains largely unreacted and becomes more detectable in the simplified matrix.

In the ZnO/geopolymer membrane (ZGH6), the XRD patterns retain the amorphous geopolymer hump, indicating that the incorporation of ZnO does not disrupt the fundamental geopolymeric network. However, additional diffraction peaks appear at  $2\theta \approx 31.7^\circ$ ,  $34.4^\circ$ , and  $47.5^\circ$ , which are characteristic of the hexagonal wurtzite structure of ZnO, corresponding to the (100), (002), and (102) planes [17], respectively. The presence of these well-defined peaks confirms the successful incorporation and crystallization of ZnO within or on the surface of the geopolymer membrane. The relatively low intensity of the ZnO peaks suggests that ZnO is well-dispersed and present in moderate loading, rather than forming large agglomerates. Importantly, the absence of new crystalline aluminosilicate phases indicates that ZnO acts primarily as a functional additive or secondary phase, rather than participating directly in the geopolymerization reaction.

The semi-quantitative analysis of the XRD patterns, as summarized in Table 1, reveals a clear evolution in the phase composition from fly ash (FA) to geopolymer membrane (GM) and ZnO-incorporated geopolymer membrane (ZGH6). The crystallinity and amorphous content were estimated using a peak deconvolution approach, in which the amorphous phase was modelled as a broad hump and the crystalline contributions were obtained from the integrated area of characteristic diffraction peaks after baseline correction. Based on this approach, FA exhibits a crystallinity of approximately  $38\pm 5\%$ , corresponding to the presence of crystalline phases such as quartz and mullite within a substantial amorphous aluminosilicate matrix. Upon geopolymerization, the crystallinity decreases significantly to  $20\pm 5\%$  in GM, while the amorphous content increases to  $80\pm 5\%$ . These results confirm the

dissolution of reactive aluminosilicate species from FA and the subsequent formation of a predominantly amorphous sodium aluminosilicate hydrate (N-A-S-H) gel, which constitutes the primary geopolymer framework.

Table 1. Semi-quantitative crystallinity and amorphous content of FA, GM, and ZGH6 from XRD data

Sample	Crystalline (%)	Amorphous (%)
FA	$38 \pm 5$	$62 \pm 5$
GM	$20 \pm 5$	$80 \pm 5$
ZGH6	$30 \pm 5$	$70 \pm 5$

In contrast, the ZGH6 sample shows a moderate increase in crystallinity to  $30\pm 5\%$ , with a corresponding decrease in amorphous content to  $70\pm 5\%$ , as presented in Table 1. This change is attributed to the incorporation of crystalline ZnO, which introduces additional small peaks without significantly altering the amorphous geopolymer network. Despite this increase, the amorphous phase remains dominant, indicating that the structural integrity of the geopolymer matrix is preserved.

The addition of  $H_2O_2$  as a pore-forming agent also influences the structure of the geopolymer network.  $H_2O_2$  decomposes into oxygen and water during synthesis, generating internal gas bubbles that induce pore formation. Some characterization, such as surface morphology, water contact angle, and porosity, was also observed in this work to validate the effect of  $H_2O_2$  as a pore-forming agent. Figure 4 shows the surface morphology of the geopolymer and ZnO/geopolymer membrane with the highest concentration of  $H_2O_2$  (ZGH6).

At lower magnification (A-1), the pristine geopolymer membrane surface appears relatively dense and compact with fewer visible pores and cracks. The compact surface morphology is typical of geopolymer structures synthesized under low-foaming conditions, where the gelation process results in a continuous aluminosilicate matrix. At higher magnification (A-2), the geopolymer surface is composed of agglomerated spherical-like particles with a relatively smooth texture, indicating a homogeneously polymerized geopolymer gel network. In addition, the fine-grained morphology observed in the SEM image

may be associated with the development of a three-dimensional aluminosilicate network during the geopolymerization.

In contrast, the ZnO/geopolymer membrane modified with 6 wt% H<sub>2</sub>O<sub>2</sub> (B-1) exhibits a visibly rougher and more porous surface morphology. The formation of microcracks and voids can be observed, likely resulting from gas evolution during the decomposition of hydrogen peroxide. H<sub>2</sub>O<sub>2</sub> acts as a pore-forming agent, releasing oxygen bubbles during the curing process that create interconnected pores within the membrane matrix [18]. This morphological transition suggests that the addition of H<sub>2</sub>O<sub>2</sub> significantly enhances surface porosity and roughness,

which can be beneficial for improving membrane permeability and reactive surface area.

At higher magnification (B-2), the presence of ZnO is evident, distributed uniformly across the geopolymer surface. The particles appear as aggregated clusters embedded in the geopolymer matrix, forming a heterogeneous texture compared to the smooth pristine surface. The ZnO particles contribute to the increased surface roughness and may also play a role in modifying the surface chemistry, enhancing hydrophilicity or photocatalytic activity depending on the intended application [19]. The interface between ZnO and the geopolymer matrix appears well integrated, indicating good adhesion and dispersion achieved during the mixing process.

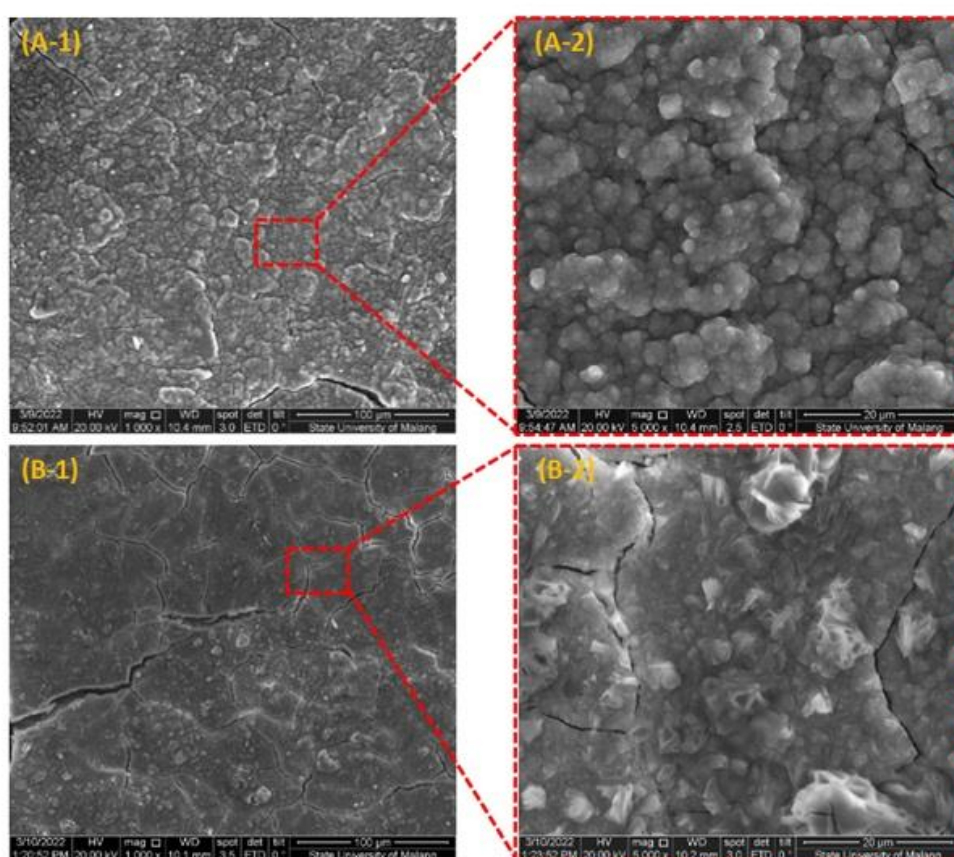


Figure 4. Surface morphology of (A) geopolymer and (B) ZnO/geopolymer membrane with magnification of (1) 1,000x and (2) 5,000x

The surface wettability of the membranes was evaluated through a water contact angle test, as shown in Figure 5. The pristine geopolymer membrane

(denoted as GM) exhibited a contact angle of approximately 21.63°, indicating its intrinsically hydrophilic nature due to the abundance of hydroxyl (-

OH) groups on the aluminosilicate surface [20]. These hydrophilic groups are capable of forming a hydrogen bond with water molecules, facilitating the rapid spreading of the water droplet over the surface.

Upon the incorporation of ZnO particles (ZGH2), the contact angle slightly decreased, suggesting an improvement in hydrophilicity. The presence of ZnO introduces additional hydroxyl groups on the surface, derived from the surface-adsorbed water and Zn-OH species, which enhance surface polarity [21]. Moreover, ZnO can increase surface roughness, and when combined with the inherently hydrophilic geopolymer matrix, this roughness amplifies the wetting behaviour according to Wenzel's model. Thus, ZnO loading not only modifies the chemical functionality of the surface but also contributes to a more water-affinitive topography [22].

A further decline in contact angle was observed with increasing H<sub>2</sub>O<sub>2</sub> concentration, confirming that the addition of H<sub>2</sub>O<sub>2</sub> enhances the hydrophilicity of the membrane surface. The

decomposition of H<sub>2</sub>O<sub>2</sub> during the synthesis generates oxygen gas, which creates more pores on the membrane surface [23]. This increased porosity leads to a higher effective surface area and a larger number of exposed hydrophilic sites. Additionally, the formation of interconnected pores enhanced capillary wetting effects, allowing water to penetrate and spread more easily across the surface.

Among all samples, the ZGH6 membrane exhibited the lowest contact angle, indicating the highest hydrophilicity. This can be attributed to the synergistic effect of ZnO addition and extensive pore formation. However, the slightly rougher and cracked morphology observed in the SEM image (Figure 4B) suggests that excessive H<sub>2</sub>O<sub>2</sub> may cause over-foaming and structural instability, which could influence long-term mechanical strength [24]. Nevertheless, in terms of wettability, the modification successfully transformed the geopolymer surface into a more water-attractive interface.

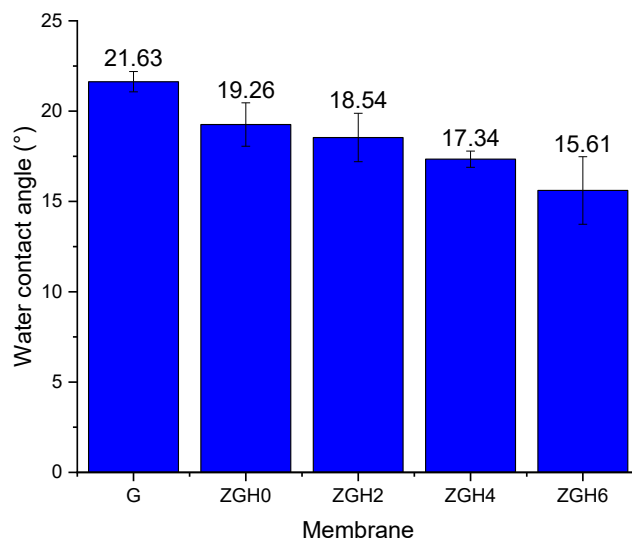


Figure 5. Surface wettability of ZnO/geopolymer membrane (n = 3)

The porosity of the geopolymer and modified ZnO/geopolymer membrane was determined using the Archimedes method, and the results are presented in Figure 6. The pristine geopolymer membrane (GM) exhibited a porosity of approximately 10%, indicating a relatively dense and compact structure. This

observation aligns well with the SEM results (Figure 4: A-1 and A-2), where the geopolymer matrix appeared smooth and less porous. The low porosity is attributed to a tightly cross-linked aluminosilicate framework formed during geopolymerization, which limits void formation and restricts fluid permeability.

After the incorporation of ZnO particles (ZGH0), the porosity slightly decreased compared to the pristine geopolymer. This reduction can be explained by the partial occupation of interstitial spaces within the geopolymer network by ZnO particles. The particles may fill or block existing micro-voids, leading to a denser composite structure. Although ZnO addition enhances surface hydrophilicity, it does not significantly contribute to pore generation when used without a pore-forming agent.

A notable increase in porosity was observed when H<sub>2</sub>O<sub>2</sub> was introduced into the synthesis system. The porosity increased progressively with H<sub>2</sub>O<sub>2</sub> concentration, ZGH2 exhibited around 30%, ZGH4 approximately 38.52%, and ZGH6 reached the highest

porosity of nearly 52%. This clear trend demonstrates that H<sub>2</sub>O<sub>2</sub> effectively acts as a pore-forming agent during membrane formation. The decomposition of H<sub>2</sub>O<sub>2</sub> releases gas bubbles, which become entrapped within the geopolymer gel matrix before escaping during curing [25]. These bubbles leave behind interconnected voids and microchannels, thus significantly enhancing the overall porosity of the membrane. The presence of more porous on the membrane architecture led to reduce mechanical integrity. Although mechanical testing was not performed in this study, Aziz et al [26] have demonstrated that geopolymer-based materials possess high compressive strength and structural integrity due to their three-dimensional aluminosilicate network.

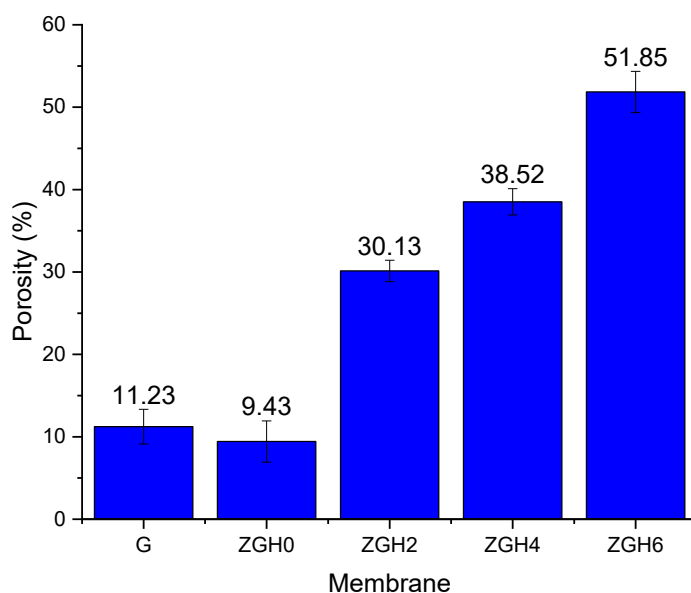


Figure 6. Porosity of all developed membranes was measured using Archimedes' method (n = 3)

This increase in porosity not only modifies the physical structure but also affects the functional performance of the membrane. Although direct water flux and filtration performance measurements were not conducted in this study, the significant increase in porosity (up to ~52%) and enhanced hydrophilicity (contact angle < 15°) strongly suggest improved water permeability. Kaliappan et al [27] have established that higher porosity and surface hydrophilic surfaces facilitate water transport and reduce fouling potential.

A higher porosity is expected to enhance the membrane's permeability and facilitate fluid transport through the interconnected pore network, which is advantageous for filtration applications. However, excessive porosity, as seen in the ZGH6 membrane, may compromise mechanical integrity, leading to the formation of cracks as observed in the SEM image (Figure 4B). Therefore, while increasing H<sub>2</sub>O<sub>2</sub> concentration is beneficial for achieving higher porosity and improved mass transfer, an optimal

balance must be maintained to ensure structural stability.

The combined results from SEM, water contact angle, and porosity measurements confirm the successful modification of the geopolymer membrane's surface and internal structure. The synergy between ZnO incorporation and controlled H<sub>2</sub>O<sub>2</sub> addition allows for the fine-tuning of the membrane characteristics, achieving both improved hydrophilicity and tailored porosity suitable for high-performance separation processes. Therefore, the performance of ZnO/geopolymer membranes will be systematically evaluated in future work.

#### 4. Conclusion

The successful fabrication of ZnO/geopolymer membrane from coal fly ash using hydrogen peroxide (H<sub>2</sub>O<sub>2</sub>) as a pore-forming agent demonstrates a sustainable approach to enhancing performance for water treatment applications. The incorporation of ZnO effectively modified the surface chemistry, increasing hydrophilicity and functional activity, while the controlled addition of H<sub>2</sub>O<sub>2</sub> generated a more porous and interconnected structure through oxygen bubble formation during curing. As the H<sub>2</sub>O<sub>2</sub> concentration increased from 0 to 6 wt%, the membrane exhibited a significant rise in porosity from 10% to 50% and a reduction in water contact angle from 25° to below 15°, confirming the tunable surface wettability and pore architecture. These synergistic effects between ZnO and H<sub>2</sub>O<sub>2</sub> not only improved surface roughness and water affinity but also offered a pathway to balance permeability and mechanical stability. Overall, this study highlights the potential of waste-derived ZnO/geopolymer membrane as an eco-friendly and high-performance material for sustainable water purification technology in the future.

#### CRedit authorship contribution statement

RMI: Writing – original draft, formal analysis, funding acquisition, supervision, conceptualization, SS: investigation, formal analysis, EPT: funding acquisition, writing – review and editing, HF: formal analysis, writing – review and editing, MANA: Data curation, formal analysis, YW: Review and editing,

SW: Writing – review & editing, DSK: formal analysis, validation

#### Declaration of Competing Interest

The authors declare that they have no known competing financial interests or personal relationships that could have appeared to influence the work reported in this paper.

#### Data availability

Data will be made available upon reasonable request.

#### Acknowledgment

The authors thank Pulang Pisau Coal Power Plant for providing the fly ash sample. We also thank to Kurita Water and Environment Foundation (KWEF), Japan for the Research Grant under scheme of Kurita Overseas Research Grant (KORG) 2025 with contract no 25Pid196.

#### References

- [1] M. R. Adam *et al.*, “Advances in adsorptive membrane technology for water treatment and resource recovery applications: A critical review,” *Journal of Environmental Chemical Engineering*, vol. 10, no. 3, p. 107633, Mar. 2022, doi: 10.1016/j.jece.2022.107633.
- [2] N. Nurlina *et al.*, “A review of geopolymer membrane for water treatment,” *Applied Clay Science*, vol. 251, p. 107301, Feb. 2024, doi: 10.1016/j.clay.2024.107301.
- [3] H. Yu, M. Xu, C. Chen, Y. He, and X. Cui, “A review on the porous geopolymer preparation for structural and functional materials applications,” *International Journal of Applied Ceramic Technology*, vol. 19, no. 4, pp. 1793–1813, Feb. 2022, doi: 10.1111/ijac.14028.
- [4] S. Shiwa, A. Khosravi, F. Mohammadi, M. Abbasi, and M. Sillanpää, “The capacity of Alkali-Activated industrial wastes in novel sustainable ceramic membranes,” *ChemBioEng Reviews*, vol. 11, no. 3, pp. 555–572, Apr. 2024, doi: 10.1002/cben.202300041.

- [5] D. Chen *et al.*, "Influence of direct foaming methods on the early performance and microstructure of metakaolin-based foam geopolymers," *International Journal of Applied Ceramic Technology*, vol. 22, no. 1, Jul. 2024, doi: 10.1111/ijac.14848.
- [6] J. Zheng *et al.*, "Rapid fabrication of porous metakaolin-based geopolymer via microwave foaming," *Applied Clay Science*, vol. 249, p. 107238, Dec. 2023, doi: 10.1016/j.clay.2023.107238.
- [7] X. Zhang, X. Zhang, X. Zhang, X. Zhang, X. Li, and M. Ma, "Bubble behaviors in chemical direct foaming process and effects on pore structures of geopolymer foams," *Journal of the American Ceramic Society*, vol. 105, no. 10, pp. 6063–6075, Jun. 2022, doi: 10.1111/jace.18591.
- [8] B. K. Dejene and T. M. Geletaw, "A review of plant-mediated synthesis of zinc oxide nanoparticles for self-cleaning textiles," *Research Journal of Textile and Apparel*, vol. 28, no. 4, pp. 879–892, Apr. 2023, doi: 10.1108/rjta-12-2022-0154.
- [9] R. M. Iqbal, "Innovative Hematite-Incorporated Geopolymer Membrane from Coal Fly Ash through Direct Foaming Method," *Materials Research Proceedings*, vol. 56, pp. 1–10, Jan. 2025, doi: 10.21741/9781644903636-1.
- [10] R. M. Iqbal *et al.*, "Fabrication and characterization of fly ash-based geopolymer and its performance for immobilization of heavy metal cations," *Communications in Science and Technology*, vol. 7, no. 2, pp. 112–118, Dec. 2022, doi: 10.21924/cst.7.2.2022.868.
- [11] H. Fansuri *et al.*, "Immobilization and leaching behavior of Cd<sup>2+</sup> and Pb<sup>2+</sup> heavy metal ions in Indonesian fly ash-based geopolymers," *Environmental Advances*, vol. 15, p. 100510, Feb. 2024, doi: 10.1016/j.envadv.2024.100510.
- [12] A. Bouchikhi *et al.*, "Advancements in Heavy Metal Stabilization: A Comparative Study on zinc Immobilization in Glass-Portland Cement Binders," *Materials*, vol. 17, no. 12, p. 2867, Jun. 2024, doi: 10.3390/ma17122867.
- [13] M. Saukani, A. N. Lisdawati, H. Irawan, R. M. Iqbal, D. M. Nurjaya, and S. Astutiningsih, "Effect of Nano-Zirconia addition on mechanical properties of Metakaolin-Based geopolymer," *Journal of Composites Science*, vol. 6, no. 10, p. 293, Oct. 2022, doi: 10.3390/jcs6100293.
- [14] J. Liu *et al.*, "Synthesis of geopolymer using municipal solid waste incineration fly ash and steel slag: Hydration properties and immobilization of heavy metals," *Journal of Environmental Management*, vol. 341, p. 118053, May 2023, doi: 10.1016/j.jenvman.2023.118053.
- [15] B. Ma *et al.*, "Assessing the viability of a high performance one-part geopolymer made from fly ash and GGBS at ambient temperature," *Journal of Building Engineering*, vol. 75, p. 106978, Jun. 2023, doi: 10.1016/j.jobbe.2023.106978.
- [16] S. Pu, Z. Zhu, W. Song, W. Huo, and C. Zhang, "An eco-friendly acid fly ash geopolymer with a higher strength," *Construction and Building Materials*, vol. 335, p. 127450, Apr. 2022, doi: 10.1016/j.conbuildmat.2022.127450.
- [17] R. M. Iqbal *et al.*, "Unravelling the effect of ZnO nanoparticles deposition via dip coating to enhance performance of PVDF-based omniphobic membrane for membrane distillation," *Surfaces and Interfaces*, vol. 59, p. 105975, Feb. 2025, doi: 10.1016/j.surfin.2025.105975.
- [18] B. Ahmad *et al.*, "Synthesis of novel fly ash based geo-polymeric membranes for the treatment of textile waste water," *International Journal of Environmental Science and Technology*, vol. 19, no. 7, pp. 6117–6126, Jul. 2021, doi: 10.1007/s13762-021-03527-4.
- [19] H. Etemadi, H. Khezraqa, and M. Hermani, "Incorporation of amino-functionalized ZnO nanoparticles into polycarbonate/polyvinyl alcohol thin-film membrane for enhanced water treatment," *Polymer Engineering and Science*, vol. 62, no. 9, pp. 2891–2899, Jul. 2022, doi: 10.1002/pen.26070.
- [20] Y. Hu, Z. Jin, B. Pang, Z. Du, X. Li, and Y. Huang, "Surface modification of geopolymer coatings with polymethylhydrosiloxane-tetraethyl orthosilicate (PMHS-TEOS) for

- inhibiting efflorescence,” *Construction and Building Materials*, vol. 446, p. 137914, Aug. 2024, doi: 10.1016/j.conbuildmat.2024.137914.
- [21] Q. Li *et al.*, “Structural characterization and surface polarity determination of polar ZnO films prepared by MBE,” *Applied Nanoscience*, vol. 13, no. 5, pp. 3197–3204, Jul. 2021, doi: 10.1007/s13204-021-01978-2.
- [22] F. U. Ahmed, D. Upadhaya, D. D. Purkayastha, and M. G. Krishna, “Stable hydrophilic and underwater superoleophobic ZnO nanorod decorated nanofibrous membrane and its application in wastewater treatment,” *Journal of Membrane Science*, vol. 659, p. 120803, Jul. 2022, doi: 10.1016/j.memsci.2022.120803.
- [23] D. Yan *et al.*, “A comparative study of porous geopolymers synthesized by pre-foaming and H<sub>2</sub>O<sub>2</sub> foaming methods: Strength and pore structure characteristics,” *Ceramics International*, vol. 50, no. 10, pp. 17807–17817, Feb. 2024, doi: 10.1016/j.ceramint.2024.02.270.
- [24] S. Benkhirat, G. Plantard, E. Ribeiro, H. Glenat, Y. Gorand, and K. Nouneh, “A way to macroporous and alveolar geopolymer foams elaboration: Influence of operating parameters on porosity characteristics,” *Results in Materials*, vol. 24, p. 100613, Aug. 2024, doi: 10.1016/j.rinma.2024.100613.
- [25] K. Khan, M. Irfan, N. U. Amin, H. Jiang, and S. Gul, “Synthesis and characterization of porous reduced graphene oxide based geopolymeric membrane with titanium dioxide coating for forward osmosis application,” *Chemosphere*, vol. 313, p. 137480, Dec. 2022, doi: 10.1016/j.chemosphere.2022.137480.
- [26] I. H. A. Aziz *et al.*, “Mechanical Performance, Microstructure, and Porosity Evolution of Fly Ash Geopolymer after Ten Years of Curing Age,” *Materials*, vol. 16, no. 3, p. 1096, Jan. 2023, doi: 10.3390/ma16031096.
- [27] S. K. Kaliappan, A. A. Siyal, Z. Man, M. Lay, and R. Shamsuddin, “Effect of pore forming agents on geopolymer porosity and mechanical properties,” *AIP Conference Proceedings*, Jan. 2018, doi: 10.1063/1.5055468.